Sloshing Response of Liquid Storage Tanks Subjected to Earthquakes with Different Peak Acceleration to Velocity Ratios

Y.S. Choun
Korea Atomic Energy Research Institute, Republic of Korea

SUMMARY:
The peak ground acceleration to velocity (A/V) ratio is utilized to characterize the significant frequency content of the input earthquake motions. This study discussed the sloshing response of rigid rectangular tanks under various earthquake ground motions with different peak A/V ratios for three types of tanks, i.e., broad, medium and tall tanks. As input motions, 75 earthquake ground motion records, with different A/V ratios, were selected from different earthquake events to represent all earthquake ground motions with various frequency contents. It is clearly revealed that the peak A/V ratio of earthquake ground motions is a significant parameter in predicting the sloshing response of liquid storage tanks. For earthquake ground motions with a high A/V ratio, the sloshing response may be negligible in the design of liquid storage tanks, while for a low A/V ratio the sloshing impact should be highly significant. It is strongly recommended that the peak A/V ratio of earthquake ground motions should be properly included in the seismic analysis and design of liquid storage tanks.

Keywords: Liquid sloshing, Rectangular tank, Peak acceleration to velocity ratio, Liquid depth/tank length ratio

1. INTRODUCTION

The earthquake-induced liquid sloshing in a tank has been of great concern for the past five decades and a number of extensive studies have been performed on the sloshing behaviour under earthquake ground excitation. Nevertheless, many liquid tanks have been severely damaged or have totally failed in past major earthquakes (Cooper 1997; Eshghi and Razzaghi 2005; Gates 1980; Hanson 1973; Haroun, Mourad and Izzeddine 1991; Hatayama 2008; Jennings 1971; Manos 1991; Manos and Clough 1985; Nielsen and Kiremidjian 1986; Rai 2003). Post-earthquake reconnaissance reports have indicated that liquid sloshing is one of the major causes of serious damage in a tank and the environment during earthquakes. For open tanks with an insufficient freeboard, liquid materials such as oil and chemical fluids may overflow into the surrounding area and result in the contamination of the soil. In the case of roof tanks, a large sloshing wave will impact the wall or roof of the tanks and may cause extensive damage or failure of the tanks.

Numerous papers have reported on the sloshing response in a rectangular tank subjected to earthquake ground motions since Housner (1963) proposed the first theoretical model to predict a sloshing response in a seismically excited rectangular tank. Nevertheless, up to now the sloshing response for earthquake excitation has not been properly predicted in many cases. The reason for this is that past research has focused only on the configuration of tanks and the dynamic properties of fluid motion even though the sloshing behaviour of a tank is very sensitive to the characteristics of the input motions as well as the configuration of the tank-liquid system (Choun and Yun 1999). Therefore, to evaluate and predict the sloshing response of liquid storage tanks reasonably, extensive investigations should be given to the effect of the characteristics of input motions on sloshing behaviour.

As one useful parameter to characterize the significant frequency content of input earthquake motions, the peak ground acceleration to velocity (A/V) ratio is utilized (Tso, Zhu and Heidebrecht 1992;

Sucuoglu et al. 1998). It is evident that significant differences in ground motion A/V ratios will be expected owing to the different faulting processes, source distances, and local geological conditions. The ground motions, exhibiting a large amplitude and very high frequency content in the strong-motion phase, generally result in high A/V ratios and very large spectral acceleration values at short periods, whereas the ground motions, containing intense, long duration acceleration pulses, will generally lead to low A/V ratios and pronounced spectral acceleration values for a moderate or long period. Normal ground motions with significant energy content over a broad range of frequencies and exhibiting a highly irregular acceleration pattern will generally have medium A/V ratios and acceleration spectra similar to the standard design spectrum (Zhu, Heidebrecht and Tso 1988).

In this study, the sloshing response of rigid rectangular tanks under various earthquake ground motions with different peak A/V ratios is discussed. Three types of tanks, i.e. broad, medium and tall tanks, are considered. As input motions, 75 earthquake ground motion records, with different A/V ratios, were selected from different earthquake events to represent all earthquake ground motions with various frequency contents. The linear and nonlinear sloshing wave heights were calculated and the effect of ground motion A/V ratio on the maximum sloshing wave heights is investigated.

2. SLOSHING ANALYSIS

A two-dimensional, partially liquid-filled rigid rectangular tank having a length L and a liquid depth d is considered. The main assumptions of the tank-liquid system are: (a) the tank is assumed to be rigid; (b) the bottom of the tank is assumed as rigidly fixed to a rigid ground; and (c) the liquid is assumed to be inviscid, incompressible, and irrotational. The effects of tank flexibility and soil-structure interaction on the sloshing behaviour are not included in the analysis.

2.1. Governing Equations

For an ideal fluid, the velocity potential $\phi(x,z,t)$ for the fluid motion satisfies the Laplace equation in the fluid domain.

$$\nabla^2\phi = 0 \quad \text{in} \quad 0 < x < L \quad \text{and} \quad -d < z < \eta \tag{2.1}$$

Eqn. 2.1 is solved with the time-dependent boundary conditions as specified below:

$$\frac{\partial\phi}{\partial x} = 0 \quad \text{on} \quad x = 0 \quad \text{and} \quad x = L \tag{2.2}$$

$$\frac{\partial\phi}{\partial z} = 0 \quad \text{on} \quad z = -d \tag{2.3}$$

$$\frac{\partial\eta}{\partial t} - \frac{\partial\phi}{\partial z} + \frac{\partial\phi}{\partial x}\frac{\partial\eta}{\partial x} = 0 \quad \text{on} \quad z = \eta \tag{2.4}$$

$$\frac{\partial\phi}{\partial t} + \frac{1}{2}\left[\left(\frac{\partial\phi}{\partial x}\right)^2 + \left(\frac{\partial\phi}{\partial z}\right)^2\right] + g\eta + \left(x - \frac{L}{2}\right)\ddot{u}_g = 0 \quad \text{on} \quad z = \eta \tag{2.5}$$

where $\ddot{u}_g$ is the horizontal ground acceleration, g is the gravitational acceleration, and η is the free surface elevation of the liquid.

The velocity potential function and free surface elevation can be expanded in terms of small perturbed parameter ε ($0 < \varepsilon < 1$) as (Choun and Yun 2002)

$$\phi(x,z,t)=\sum_{n=1}^{\infty}\varepsilon^n\phi_n(x,z,t) \tag{2.6}$$

$$\eta(x,t)=\sum_{n=1}^{\infty}\varepsilon^n\eta_n(x,t). \tag{2.7}$$

Substituting Eqns. 2.6 and 2.7 into two free surface boundary conditions, Eqns. 2.4 and 2.5, and replacing $\ddot{u}_g$ with $\varepsilon\ddot{X}$, Eqns. 2.8 and 2.9 are derived.

$$\begin{aligned}\left[\varepsilon\frac{\partial\eta_1}{\partial t}+\varepsilon^2\frac{\partial\eta_2}{\partial t}+\cdots\right]-\left[\varepsilon\frac{\partial\phi_1}{\partial z}+\varepsilon^2\frac{\partial\phi_2}{\partial z}+\cdots\right]\\ +\left[\varepsilon\frac{\partial\phi_1}{\partial x}+\varepsilon^2\frac{\partial\phi_2}{\partial x}+\cdots\right]\left[\varepsilon\frac{\partial\eta_1}{\partial x}+\varepsilon^2\frac{\partial\eta_2}{\partial x}+\cdots\right]\end{aligned} \tag{2.8}$$

$$\begin{aligned}\left[\varepsilon\frac{\partial\phi_1}{\partial t}+\varepsilon^2\frac{\partial\phi_2}{\partial t}+\cdots\right]+\frac{1}{2}\left[\left(\varepsilon\frac{\partial\phi_1}{\partial x}+\varepsilon^2\frac{\partial\phi_2}{\partial x}+\cdots\right)^2+\left(\varepsilon\frac{\partial\phi_1}{\partial z}+\varepsilon^2\frac{\partial\phi_2}{\partial z}+\cdots\right)^2\right]\\ +g\left[\varepsilon\eta_1+\varepsilon^2\eta_2+\cdots\right]+\varepsilon\left(x-\frac{L}{2}\right)\ddot{X}=0\end{aligned} \tag{2.9}$$

The higher-order terms may be negligible because the higher orders of ε will be close to zero. Using the two low-order terms only, i.e., terms including ε and ε^2, and applying the Taylor series, the first- and second-order governing equations are obtained.

The first-order governing equations are

$$\frac{\partial\eta_1}{\partial t}=\frac{\partial\tilde{\phi}_1}{\partial z} \tag{2.10}$$

$$\frac{\partial\tilde{\phi}_1}{\partial t}+g\eta_1=-\left(x-\frac{L}{2}\right)\ddot{X}. \tag{2.11}$$

The second-order governing equations are

$$\frac{\partial\eta_2}{\partial t}=\frac{\partial\tilde{\phi}_2}{\partial z}+\eta_1\frac{\partial^2\tilde{\phi}_1}{\partial z^2}-\frac{\partial\tilde{\phi}_1}{\partial x}\frac{\partial\eta_1}{\partial x} \tag{2.12}$$

$$\frac{\partial\tilde{\phi}_2}{\partial t}+g\eta_2=-\eta_1\frac{\partial^2\tilde{\phi}_1}{\partial t\partial z}-\frac{1}{2}\left[\left(\frac{\partial\tilde{\phi}_1}{\partial x}\right)^2+\left(\frac{\partial\tilde{\phi}_1}{\partial z}\right)^2\right]. \tag{2.13}$$

The terms with a tilde represent the differential at $\eta = 0$.

2.2. Linear Sloshing Analysis

The linear surface wave of liquid is derived by the first-order governing equations. The velocity potential satisfying the continuity condition in the fluid domain, and the boundary conditions at the walls and the bottom of the tank, can be expressed as

$$\phi_1(x,z,t)=\sum_{n=1}^{\infty}\dot{a}_n(t)\cos k_n x\cosh k_n(z+d), \tag{2.14}$$

where $\dot{a}_n(t)$ represents the derivative of $a_n(t)$, the time-dependent function associated with the surface

wave amplitude, with respect to time *t*; and k_n is the wave number obtained as $k_n = n\pi/L$.
The equation of motion can be derived from Eqns. 2.10 and 2.11 as

$$\ddot{a}_n(t) + 2\xi_n\omega_n\dot{a}_n(t) + \omega_n^2 a_n(t) = \frac{2\left[1-(-1)^n\right]}{Lk_n^2\cosh k_n d}\ddot{X}(t), \tag{2.15}$$

where ξ_n is the modal damping ratio, and $\omega_n = \sqrt{gk_n\tanh k_n d}$.
Time-dependent function $a_n(t)$ is given by

$$a_n(t) = \frac{2\left[1-(-1)^n\right]}{Lk_n^2\omega_{Dn}\cosh k_n d}\int_0^t \ddot{X}(\tau)e^{-\xi_n\omega_n(t-\tau)}\sin\omega_{Dn}(t-\tau)d\tau, \tag{2.16}$$

where $\omega_{Dn} = \omega_n\sqrt{1-\xi_n^2}$.
Thus, the linear free surface wave height can be determined by

$$\eta_1(x,t) = \sum_{n=1}^{\infty} a_n(t)k_n\cos k_n x\sinh k_n d. \tag{2.17}$$

2.3 Nonlinear Sloshing Analysis

The nonlinear surface wave of a liquid can be derived by the second-order governing equations. The velocity potential can be expressed as

$$\phi_2(x,z,t) = \sum_{n=1}^{\infty} b_n(t)\cos k_n x\cosh k_n(z+d), \tag{2.18}$$

where $b_n(t)$ represents the time-dependent function associated with the surface wave amplitude and k_n is the wave number.
An equation of motion can be derived from Eqns. 2.12 and 2.13 as

$$\ddot{b}_i(t) + 2\xi_i\omega_i\dot{b}_i(t) + \omega_i^2 b_i(t) = \frac{2}{L\cosh k_i d}q_i(t), \tag{2.19}$$

where

$$\begin{aligned} q_i(t) = {} & g\sum_{n=1}^{\infty}\sum_{m=1}^{\infty} a_n(t)\dot{a}_m(t)k_n^2 k_m\sinh k_n d\cosh k_m d\int_0^L \sin k_n x\sin k_m x\cos k_i x dx \\ & - g\sum_{n=1}^{\infty}\sum_{m=1}^{\infty} a_n(t)\dot{a}_m(t)k_n k_m^2\sinh k_n d\cosh k_m d\int_0^L \cos k_n x\cos k_m x\cos k_i x dx \\ & - 2\sum_{n=1}^{\infty}\sum_{m=1}^{\infty} \dot{a}_n(t)\ddot{a}_m(t)k_n k_m\sinh k_n d\sinh k_m d\int_0^L \cos k_n x\cos k_m x\cos k_i x dx \\ & - \sum_{n=1}^{\infty}\sum_{m=1}^{\infty} a_n(t)\ddot{a}_m(t)k_n k_m\sinh k_n d\sinh k_m d\int_0^L \cos k_n x\cos k_m x\cos k_i x dx \\ & - \sum_{n=1}^{\infty}\sum_{m=1}^{\infty} \dot{a}_n(t)\ddot{a}_m(t)k_n k_m\cosh k_n d\cosh k_m d\int_0^L \sin k_n x\sin k_m x\cos k_i x dx \end{aligned} \tag{2.20}$$

and ξ_i is the modal damping ratio, $\omega_i = \sqrt{gk_i\tanh k_i d}$.

Time-dependent function $b_i(t)$ is given by

$$b_i(t)=\frac{2}{L\omega_{Di}\cosh k_i d}\int_0^t q_i(\tau)e^{-\xi_i\omega_i(t-\tau)}\sin\omega_{Di}(t-\tau)d\tau. \tag{2.21}$$

Thus, the wave height owing to the nonlinear behaviour of the free surface can be determined by

$$\begin{aligned}\eta_2(x,t)=-\frac{1}{g}\Bigg[&\sum_{n=1}^{3}\dot{b}_n(t)\cos k_n x\cosh k_n d\\&+\sum_{n=1}^{\infty}\sum_{m=1}^{\infty}a_n(t)\ddot{a}_m(t)k_n k_m\cos k_n x\cos k_m x\sinh k_n d\sinh k_m d\\&+\frac{1}{2}\left\{\left(\sum_{n=1}^{\infty}\dot{a}_n(t)k_n\sin k_n x\cosh k_n d\right)^2+\left(\sum_{n=1}^{\infty}\dot{a}_n(t)k_n\cos k_n x\sinh k_n d\right)^2\right\}\Bigg].\end{aligned} \tag{2.22}$$

In Eqn. 2.22, only three terms are taken into account as the effect of higher modes may be neglected. The final free surface wave height can be calculated by

$$\begin{aligned}\eta(x,t)&\approx\varepsilon\eta_1(x,t)+\varepsilon^2\eta_2(x,t)\\&=-\frac{1}{g}\Bigg[\left(x-\frac{L}{2}\right)\ddot{u}_g(t)+\sum_{n=1}^{\infty}\ddot{A}_n(t)\cos k_n x\cosh k_n d+\sum_{n=1}^{3}\dot{B}_n(t)\cos k_n x\cosh k_n d\\&\quad+\sum_{n=1}^{\infty}\sum_{m=1}^{\infty}A_n(t)\ddot{A}_m(t)k_n k_m\cos k_n x\cos k_m x\sinh k_n d\sinh k_m d\\&\quad+\frac{1}{2}\left\{\left(\sum_{n=1}^{\infty}\dot{A}_n(t)k_n\sin k_n x\cosh k_n d\right)^2+\left(\sum_{n=1}^{\infty}\dot{A}_n(t)k_n\cos k_n x\sinh k_n d\right)^2\right\}\Bigg],\end{aligned} \tag{2.23}$$

where

$$A_n(t)=\varepsilon\,a_n(t)=\frac{2\left[1-(-1)^n\right]}{Lk_n^2\omega_{Dn}\cosh k_n d}\int_0^t\ddot{u}_g(\tau)e^{-\xi_n\omega_n(t-\tau)}\sin\omega_{Dn}(t-\tau)d\tau \tag{2.24}$$

$$B_n(t)=\varepsilon^2 b_n(t)=\frac{2}{L\omega_{Dn}\cosh k_n d}\int_0^t Q_n(\tau)e^{-\xi_n\omega_n(t-\tau)}\sin\omega_{Dn}(t-\tau)d\tau \tag{2.25}$$

in which $\omega_{Dn}=\omega_n\sqrt{1-\xi_n^2}$, $Q_n(t)=\varepsilon^2 q_n(t)$.

3. GROUND MOTION INPUT

The peak ground acceleration (PGA) and peak ground velocity (PGV) are usually caused by seismic waves of different frequencies. In general, the PGA is associated with high frequency waves, whereas the PGV is related to moderate or low-frequency waves. Because of the frequency-dependent attenuation of seismic waves, PGA attenuates more rapidly with distance than PGV. As a result, one would expect that ground motions near an earthquake source have higher A/V ratios than ground motions at a long distance from the source of the seismic energy release (Tso, Zhu and Heidebrecht 1992). This study selected 75 earthquake ground motions with a broad range of A/V ratios to cover both near-field and far-field ground motions as well as normal ground motions.

The earthquake records were obtained from 9 different earthquake events with magnitudes ranging from 6.1 to 7.6. The selected records have epicentral distances ranging from 7.1 to 69.1 km, original PGAs ranging from 0.084 to 1.585 g, and peak A/V ratios from 0.16 to 3.81 g/m/s.

Fig. 3.1 represents the relations between the peak acceleration and peak velocity of 75 earthquake records for different peak A/V ratios. Twenty-five records have A/V ratios lower than 0.5 g/m/s, twenty-five records are greater than 1.0 g/m/s, and twenty-five records are between 0.5 and 1.0 g/m/s.

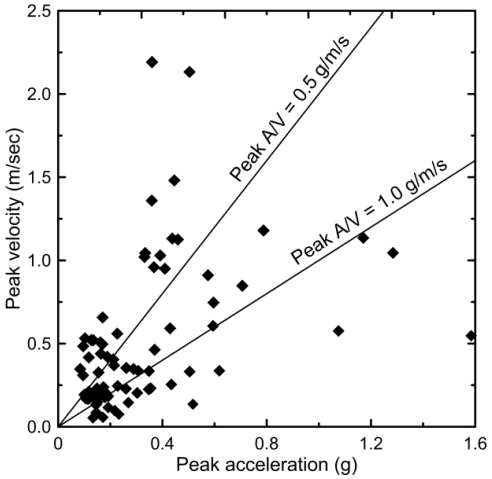

Figure 3.1. Peak acceleration versus peak velocity for different A/V ratios

Fig. 3.2(a) represents the 0.5% damped acceleration response spectra for the whole ensemble of 75 records normalized to PGA = 0.2 g. It was revealed that there are significantly different energy contents over low frequencies for earthquake records with different peak A/V ratios when they are scaled to a common peak acceleration. The low A/V ratio of earthquake records has the highest spectral acceleration, whereas the high A/V ratio has the lowest in a frequency lower than about 5 Hz. The earthquake records with low A/V ratios are rich in low frequency contents. Fig. 3.2(b) shows a 0.5% damped acceleration response spectra normalized to PGV = 0.2 m/s. The high A/V ratio of earthquake records has the highest spectral acceleration, whereas the low A/V ratio has the lowest in a frequency higher than about 2 Hz. This shows that the earthquake records with high A/V ratios are rich in high-frequency contents.

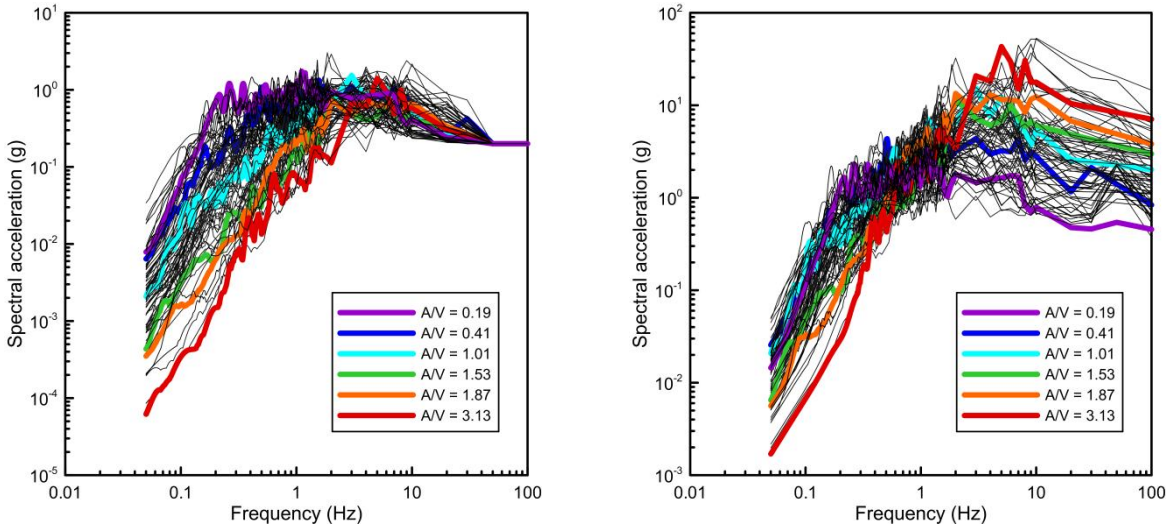

(a) Normalized to PGA = 0.2 g (b) Normalized to PGV = 0.2 m/s

Figure 3.2. 0.5% damped acceleration response spectra for selected earthquake records

4. SLOSHING RESPONSES

The sloshing response of rectangular liquid tanks depends on the liquid depth/tank length (*d/L*) ratio.

In a broad tank with a low *d/L* ratio, most of the fluid participates in the sloshing motion. On the other hand, for a tall tank with a high *d/L* ratio, only the upper portion of the fluid participates in the sloshing motion. Therefore, the sloshing response is more significant in a broad tank than in a tall tank. In this study, three types of liquid tanks are considered: a broad tank (*d/L* = 0.5; 6 m (*L*) × 3 m (*d*)), a medium tank (*d/L* = 1.0; 4 m (*L*) × 4 m (*d*)), and a tall tank (*d/L* = 2.0; 3 m (*L*) × 6 m (*d*)). The sloshing analysis used 10 sloshing modes, because sufficient higher modes have to be taken into account in the analysis for the ground excitations, particularly dominated by low-frequency contents (Choun and Yun 1999). The modal damping ratio of 0.005 is assumed for all modes.

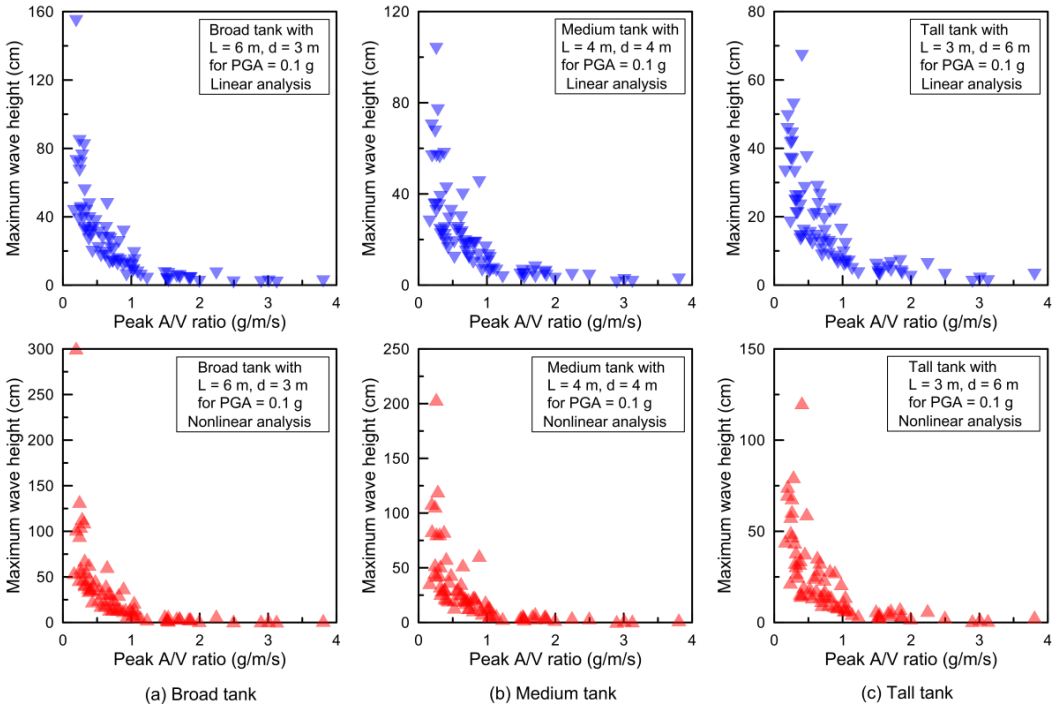

Figure 4.1. Maximum wave heights in different tanks for various A/V ratios under PGA = 0.1 g

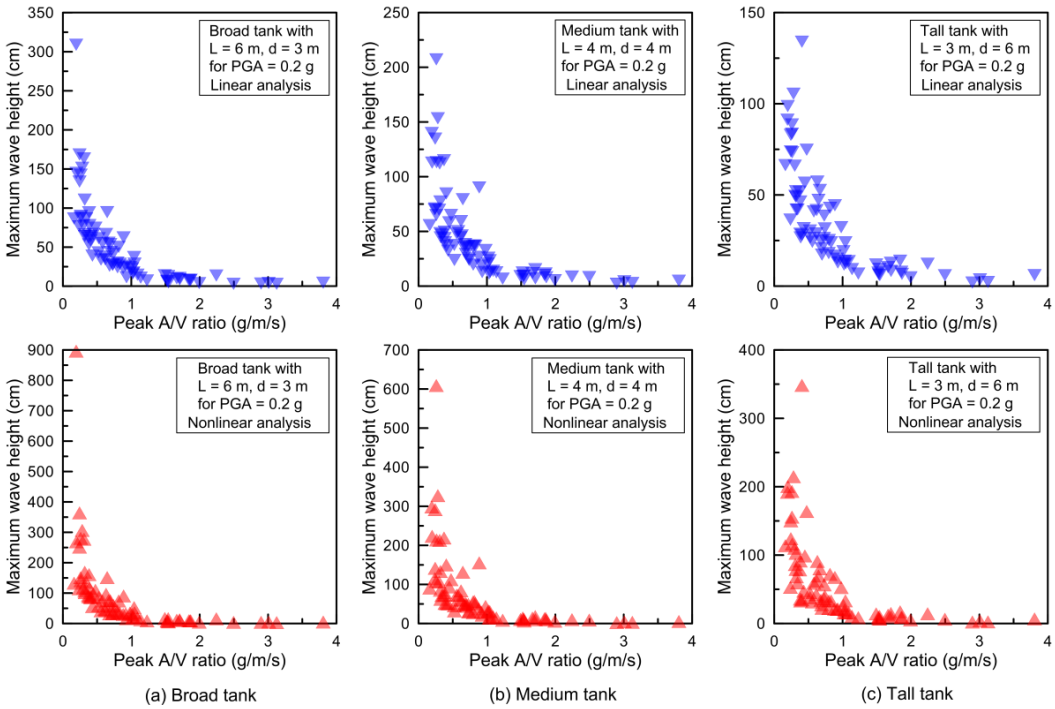

Figure 4.2. Maximum wave heights in different tanks for various A/V ratios under PGA = 0.2 g

Figs. 4.1 and 4.2 show the maximum wave heights at the walls of three types of tanks for various A/V ratios under PGAs of 0.1 g and 0.2 g, respectively. It is clearly revealed that the maximum sloshing wave heights in liquid tanks are significantly dependent upon the peak A/V ratio of the input motions. For the three types of tanks, the maximum sloshing wave heights have a tendency to decrease rapidly with an increase in the peak A/V ratio. The decrease in the broad tank is more rapid than in the tall tank. It was also found that the maximum wave heights in the three types of tanks are significant for input motions with low A/V ratios, whereas it is small for input motions with large A/V ratios under the same PGA. In particular, for a peak A/V ratio of lower than 0.5 g/m/s, the maximum wave height is remarkable. In a broad tank, the free surface of liquid may be dramatically amplified owing to the very low A/V ratio of the ground excitations. Moreover, the amplification of the free surface must be greatly increased with an increase in the peak acceleration. Thus, with an increase in the PGA, a nonlinear analysis is inevitable. For a tall tank, the maximum wave heights are not significant under a low PGA, but they increase greatly under a high PGA. For the three types of tanks, the maximum wave heights are small for a peak A/V ratio greater than about 1.0 g/m/s. Accordingly, the difference between the maximum wave heights by linear and nonlinear analyses are not large. It should be noted that the sloshing response for a ground motion with low peak acceleration and low A/V ratio may be greater than for a ground motion with a high peak acceleration and high A/V ratio.

Fig. 4.3 shows all of the results by the nonlinear analysis and the wave height ratios for various A/V ratios. The wave height ratio is defined as the ratio of maximum wave height from a nonlinear analysis to that from a linear analysis. Regardless of the types of tanks, the peak A/V ratios can be classified into three groups according to the sloshing response in the liquid storage tanks as $A/V \leq 0.5$ g/m/s, 0.5 g/m/s $< A/V \leq 1.0$ g/m/s, and $A/V > 1.0$ g/m/s. Generally, for $A/V \leq 0.5$ g/m/s, the wave height response amplifies significantly and has large variability, whereas for $A/V > 1.0$ g/m/s, the wave height response is small and nearly constant.

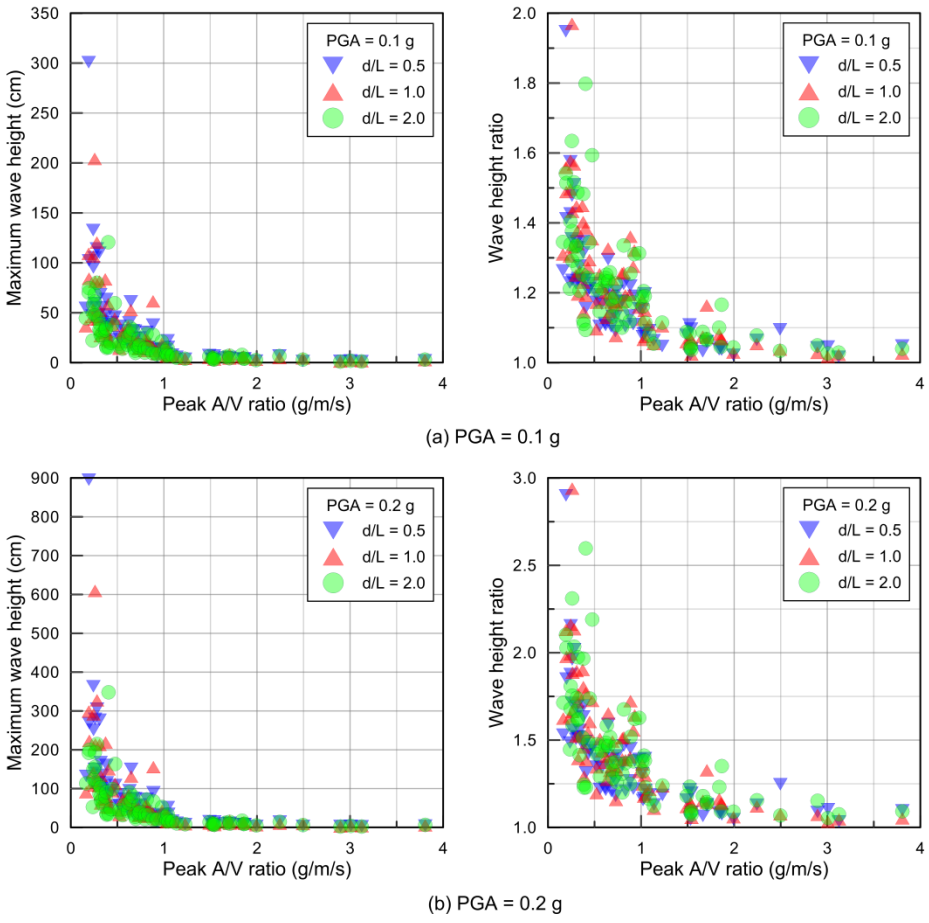

Figure 4.3. Maximum wave heights and wave height ratios of tanks for various A/V ratios under different PGAs

The amplification factors of the highest and lowest wave height response for the three A/V range groups are presented in Table 4.1. The amplification factors are obtained by dividing the wave heights with the wave heights for A/V > 1.0 g/m/s. For A/V ≤ 0.5 g/m/s, the amplification factors increase with an increase in the level of PGA. They are larger in broad and medium tanks than in a tall tank. The amplification factors for the lowest wave heights are much larger than those for the highest heights.

Table 4.1. Amplification Factors of the Wave Height Response

Tank type		PGA (g)	A/V ≤ 0.5	0.5 < A/V ≤ 1.0	A/V > 1.0
Broad tank	High	0.1	13.4	2.7	1.0
		0.2	17.2	2.9	1.0
	Low	0.1	15.7	4.6	1.0
		0.2	17.9	5.1	1.0
Medium tank	High	0.1	14.0	4.2	1.0
		0.2	18.9	4.8	1.0
	Low	0.1	18.7	7.7	1.0
		0.2	20.8	8.8	1.0
Tall tank	High	0.1	8.4	2.5	1.0
		0.2	10.5	2.7	1.0
	Low	0.1	14.8	8.5	1.0
		0.2	14.9	9.4	1.0

Table 4.2 shows the wave height ratios for the three A/V range groups. This indicates that the difference between the two results from the linear and nonlinear analyses is significant for A/V ≤ 0.5 g/m/s and the difference under PGA = 0.2 g becomes twice the difference under PGA = 0.1 g. Thus, for A/V ≤ 0.5 g/m/s, a nonlinear analysis must be carried out. For 0.5 g/m/s < A/V ≤ 1.0 g/m/s, a nonlinear analysis is recommended since the difference becomes significant under a high PGA. For A/V > 1.0 g/m/s, a linear analysis is acceptable because the sloshing wave heights are relatively small.

Table 4.2. Wave Height Ratios in Different Tanks and PGAs

Tank type	PGA (g)	A/V ≤ 0.5		0.5 < A/V ≤ 1.0		A/V > 1.0	
		Low	High	Low	High	Low	High
Broad tank	0.1	1.16	1.95	1.09	1.30	1.02	1.20
	0.2	1.31	2.90	1.18	1.59	1.04	1.40
Medium tank	0.1	1.14	1.97	1.08	1.36	1.02	1.18
	0.2	1.29	2.94	1.16	1.72	1.03	1.36
Tall tank	0.1	1.09	1.80	1.10	1.34	1.03	1.20
	0.2	1.23	2.60	1.20	1.68	1.05	1.41

5. CONCLUSIONS

The sloshing responses of rectangular liquid storage tanks for input motions with different ground motion A/V ratios are investigated in this study. Linear and nonlinear sloshing analyses, which use a perturbation approach, are carried out to identify the effect of the peak A/V ratio on nonlinear responses.

It is clearly revealed that the peak A/V ratio of earthquake ground motions is a significant parameter in predicting the sloshing response of liquid storage tanks. Regardless of the types of tanks, the peak A/V ratios can be classified into three groups according to the sloshing response in liquid storage tanks as A/V ≤ 0.5 g/m/s, 0.5 g/m/s < A/V ≤ 1.0 g/m/s, and A/V > 1.0 g/m/s. For input ground motions with the peak A/V ≤ 0.5 g/m/s, the sloshing response is significant in the three types of tanks, i.e., a broad tank, medium tank, and tall tank. The results by a nonlinear analysis are much larger than those by a linear analysis. In particular, tremendous sloshing responses may occur in the broad tank under a strong ground motion. Therefore, a nonlinear analysis must be used in calculating the sloshing responses for

input ground motions with a peak A/V ≤ 0.5 g/m/s. For input ground motions with 0.5 g/m/s < A/V ≤ 1.0 g/m/s, a sloshing response is not significant. The results by a nonlinear analysis are a little larger than those by a linear analysis. However, a nonlinear analysis is recommended as a significant response may occur under a high PGA. For input ground motions with a peak A/V > 1.0 g/m/s, the sloshing response is relatively small in the three types of tanks. Thus, a linear analysis may be sufficient for calculating sloshing responses.

The sloshing behavior in a liquid tank depends on the PGV, as well as on the PGA of earthquake ground motions. According to the discussion in this study, the peak A/V ratio must be considered as a significant seismic hazard parameter in addition to the PGA in the seismic design of liquid storage tanks. Obviously, for earthquake ground motions with a high A/V ratio, the sloshing response may be negligible in the design of liquid storage tanks, while for those with low A/V ratios the sloshing impact should be considerable. Nevertheless, the current seismic design codes and standards on liquid-containing tanks do not take into account the peak A/V ratio to determine the seismic design forces (Jaiswal, Rai and Jain 2007). Therefore, it is strongly recommended that the peak A/V ratio of earthquake ground motions should be properly included in the seismic analysis and design procedures of liquid storage tanks.

REFERENCES

Choun, Y.S. and Yun, C.B. (1999). Sloshing analysis of rectangular tanks with a submerged structure by using small-amplitude water wave theory. *Earthquake Engineering and Structural Dynamics* **28:7**,763-783.

Choun, Y.S. and Yun, C.B. (2002). Nonlinear analysis of sloshing in rectangular tanks by perturbation approach. *Journal of the Earthquake Engineering Society of Korea* **6:6**,55-64. (in Korean)

Cooper, T.W. (1997). A Study of the Performance of Petroleum Storage Tanks during Earthquake 1933-1995. National Institute of Standards and Technology. Report No. NIST GCR 97-720.

Eshghi, S. and Razzaghi, M. (2005). Performance of industrial facilities in the 2003 Bam, Iran, Earthquake. *Earthquake Spectra* **21:S1**,395-410.

Gates, W.E. (1980). Elevated and Ground-Supported Steel Storage Tanks. Reconnaissance Report, Imperial County, California Earthquake of October 15, 1979. Earthquake Engineering Research Institute, Oakland, California, U.S.A.

Hanson, R.D. (1973). Behaviour of Liquid Storage Tanks, The Great Alaska Earthquake of 1964. *Proceedings of the National Academy of Science*. **Vol 7:** 331-339.

Haroun, M.A., Mourad, S.A. and Izzeddine, W. (1991). Performance of Liquid Storage Tanks during the 1989 Loma Prieta Earthquake. *Proceedings of Lifeline Earthquake Engineering*. ASCE. 1152-1160.

Hatayama, K. (2008). Lessons from the 2003 Tokachi-oki, Japan, Earthquake for prediction of long-period strong ground motions and sloshing damage to oil storage tanks. *Journal of Seismology* **12:2**,255-263.

Housner, G.W. (1963). The dynamic behavior of water tanks. *Bulletin of the Seismological Society of America* **53:2**,381-387.

Jaiswal, O.R., Rai, D.C. and Jain, S.K. (2007). Review of seismic codes on liquid-containing tanks. *Earthquake Spectra* **23:1**,239-260.

Jennings, P.E. (ed.). (1971). Engineering Features of the San Fernando Earthquake of Feb 9, 1971. California Institute of Technology. Report No. EERL-71-02:434-470.

Manos, G.C. (1991). Evaluation of the earthquake performance of anchored wine tanks during the San Juan, Argentina, 1977 Earthquake. *Earthquake Engineering and Structural Dynamics* **20:12**,1099-1114.

Manos, G.C. and Clough, R.W. (1985). Tank damage during the May 1983 Coalinga, California Earthquake. *Earthquake Engineering and Structural Dynamics* **13:4**,449-466.

Nielsen, R. and Kiremidjian, A.S. (1986). Damage to oil refineries from major earthquakes. *Journal of Structural Engineering* **112:6**,1481-1491.

Rai, D.C. (2003). Performance of Elevated Tanks in Mw 7.7 Bhuj Earthquake of January 26th, 2001. *Proceedings of Indian Academy of Science*. **112:3**,421-429.

Sucuoglu, H., Yücemen, S., Gezer, A. and Erberik, A. (1998). Statistical evaluation of the damage potential of earthquake ground motions. *Structural Safety* **20:4**,357-378.

Tso, W.K., Zhu, T.J. and Heidebrecht, A.C. (1992). Engineering implication of ground motion A/V ratio. *Soil Dynamics and Earthquake Engineering* **11:3**,133-144.

Zhu, T.J., Heidebrecht, A.C. and Tso, W.K. (1988). Effect of peak ground acceleration to velocity ratio on ductility demand of inelastic systems. *Earthquake Engineering and Structural Dynamics* **16:1**,63-79.